



# Evapotranspiration and its components over a rainfed spring maize cropland under plastic film on the Loess Plateau, China

Xiang Gao (Gao, X)<sup>1,2</sup>, Fengxue Gu (Gu, FX)<sup>1</sup>, Daozhi Gong (Gong, DZ)<sup>1</sup>, Weiping Hao (Hao, WP)<sup>1</sup>, Jianmin Chu (Chu, JM)<sup>2</sup>, and Haoru Li (Li, HR)<sup>1</sup>

<sup>1</sup>Key Laboratory of Dryland Agriculture, Ministry of Agriculture and Rural Affairs of the People's Republic of China, Beijing 100081, China

<sup>2</sup>Key Laboratory of Tree Breeding and Cultivation of National Forestry and Grassland Administration, Research Institute of Forestry, Chinese Academy of Forestry, Beijing 100091, China

## Abstract

**Aim of study:** To determine seasonal variations in evapotranspiration (ET) and its components; and ascertain the key factors controlling ET and its components in a rainfed spring maize field under plastic film.

**Area of study:** Shouyang County in Shanxi Province on the eastern Loess Plateau, China

**Material and methods:** Eddy covariance system combined with micro-lysimeters and meteorological observing instruments were used in the field. The manual method was used to measure the green leaf area index (GLAI) during the growing season.

**Main results:** In 2015 and 2016, the growing season ET accounted for 80% and 79% of annual ET, respectively. Soil evaporation (E) accounted for 36% and 33% of the growing season ET in 2015 and 2016, respectively. The daily crop coefficient increased with increasing GLAI until a threshold of  $\sim 3 \text{ m}^2 \text{ m}^{-2}$  in the canopy-increasing stage, and decreased linearly with decreasing GLAI in the canopy-decreasing stage. At equivalent GLAI, daily basal crop coefficient and soil water evaporation coefficient were generally higher in the canopy-increasing and -decreasing stages, respectively. During the growing season, the most important factor controlling daily ET, T, and E was net radiation ( $R_n$ ), followed by GLAI for daily ET and T, and soil water content at 10-cm depth for daily E; during the non-growing season, daily ET was mainly controlled by  $R_n$ .

**Research highlights:** The daily crop coefficient and its components reacted differently to GLAI in the canopy-increasing and -decreasing stages.

**Additional key words:** evapotranspiration partitioning; influence factors; water balance; crop coefficient and its components.

**Abbreviations used:** E (soil evaporation); ET (evapotranspiration); ET<sub>0</sub> (reference crop evapotranspiration); GLAI (green leaf area index);  $H_a$  (air relative humidity);  $K_c$  (crop coefficient);  $K_{cb}$  (basal crop coefficient);  $K_e$  (soil water evaporation coefficient); P (precipitation);  $R_n$  (net radiation); SWC (soil water content at 10-cm depth); T (crop transpiration);  $T_a$  (air temperature); U (wind speed); VPD (vapor pressure deficit).

**Authors' contributions:** Conceived and designed the experiments: FG, DG, and WH. Performed the experiments: HL and XG. Wrote the paper: XG and JC. All authors read and approved the final article.

**Citation:** Gao, X; Gu, FX; Gong, DZ; Hao, WP; Chu, JM; Li, HR (2020). Evapotranspiration and its components over a rainfed spring maize cropland under plastic film on the Loess Plateau, China. Spanish Journal of Agricultural Research, Volume 18, Issue 4, e1205. <https://doi.org/10.5424/sjar/2020184-16370>

**Received:** 10 Jan 2020. **Accepted:** 03 Nov 2020.

**Copyright** © 2020 INIA. This is an open access article distributed under the terms of the Creative Commons Attribution 4.0 International (CC-by 4.0) License.

Funding agencies/institutions	Project / Grant
Fundamental Research Funds for the Central Non-profit Research Institution of CAF, China	CAFYBB2019SY007
Research Funding of Key Laboratory of Dryland Agriculture, China	2018K LDA01
Central Public-interest Scientific Institution Basal Research Fund, China	BSRF201708

**Competing interests:** The authors have declared that no competing interests exist.

**Correspondence** should be addressed to Xiang Gao: [gaoxiang@caf.ac.cn](mailto:gaoxiang@caf.ac.cn) or Weiping Hao: [haoweiping@caas.cn](mailto:haoweiping@caas.cn) (shared corresponding authors).

## Introduction

The evapotranspiration (ET) is coupled with photosynthesis, and plays a key role in the energy balance of land

surface (Wu & Shukla, 2014), thereby affecting many biological and physical processes that occur at the ground surface (Sen, 2004). The ET at vegetation surfaces have important effects on several aspects of climate (Wever

*et al.*, 2002). In turn, ET is affected by the soil properties, vegetation characteristics, and weather (Suyker & Verma, 2008; Ding *et al.*, 2013; Yang *et al.*, 2013). More than 80% of total cultivated land is rainfed cropland (FAO, 2011), which plays a vital role in maintaining stable ecosystems and agricultural productivity (Zhang *et al.*, 2016). It is critical, therefore, to study ET in rainfed agricultural ecosystems to model crop production and to elucidate the mechanisms for the hydrological and biogeochemical cycles.

In recent decades, the eddy covariance system is regarded as the standard method for observing turbulent fluxes between the surface and atmosphere (Taylor *et al.*, 2013). This technique has also been widely used for accurate measurements of water vapor fluxes in different terrestrial ecosystems (Wu & Shukla, 2014; Yang *et al.*, 2016). Published studies on ET in croplands focused mainly on irrigation croplands (Li *et al.*, 2008; Yuan *et al.*, 2014), while researchers have paid less attention to rainfed croplands (Suyker & Verma, 2009). Soil evaporation (E) and crop transpiration (T) constitute most ET in agricultural ecosystems; understanding these two components is important for optimizing agricultural management to increase plants water use efficiency (Kool *et al.*, 2014). Considerable research on how abiotic and biotic factors control ET and its components is needed in rainfed croplands. The crop coefficient ( $K_c$ ), and its components, soil water evaporation coefficient ( $K_e$ ) and basal crop coefficient ( $K_{cb}$ ), are the most important parameters for describing ET and its components (Alberto *et al.*, 2014). Because  $K_c$  and its components can be used to estimate ET and its components (Zhao *et al.*, 2015; Miao *et al.*, 2016), they should be determined in rainfed agricultural ecosystems (Suyker & Verma, 2009; Liu *et al.*, 2010a). ET in the non-growing season influences the annual water balance (Suyker & Verma, 2009; Zhang *et al.*, 2016), as this period usually lasts more than half a year, but few studies have paid attention to this period in single-cropping systems in the drylands of northwest China.

The Loess Plateau has a population of ~90 million and covers an area of approximately 9 degrees of latitude and 11 degrees of longitude with a semiarid monsoon climate in northwest China (Liu *et al.*, 2010b). As surface runoff is sparse and groundwater is deep, the Plateau is an important rainfed agricultural region, especially considering the rapid degradation of fragile ecosystems in China. Spring maize (*Zea mays* L.), the dominant crop on the Plateau, has an important influence on regional food security (Bu *et al.*, 2013). However, low temperatures and limited water in April–June usually result in crop growth retardation (Liu *et al.*, 2009; 2010b). Plastic film mulching has been widely used in spring maize croplands on the Plateau because it can significantly increase soil water and heat conditions during the early growing season and increase grain yields (Liu *et al.*, 2009, 2010b; Bu *et al.*, 2013). To date,

there have been few studies using eddy covariance techniques for year-round ET in rainfed spring maize croplands under plastic film.

In this study, a rainfed spring maize field under plastic film was investigated using the eddy covariance system combined with micro-lysimeters at Shouyang site in 2015 and 2016. The study objectives were limited to: (i) determine seasonal variations in ET and its components; and (ii) ascertain the key factors controlling ET and its components in the field on the Loess Plateau.

## Material and methods

### Site description

The experiments were conducted in a typical rainfed cropland on the eastern Loess Plateau, located in Shouyang County in Shanxi Province (N 37°45', E 113°12', altitude 1,202 m). The study area is characterized by a semi-arid temperate continental monsoon climate. Mean annual precipitation is 474.5 mm, with over 70% occurring from July–September; mean annual temperature is 8.2 °C and the mean annual frost-free period is 150 days. The soil is sandy-loamy, containing 54.9% sand, 29.5% silt and 15.6% clay; the soil bulk density is 1.34 g cm<sup>-3</sup>. The contents of soil organic matter, total nitrogen, total phosphorus, and total potassium are 9.00 g kg<sup>-1</sup>, 0.79 g kg<sup>-1</sup>, 0.72 g kg<sup>-1</sup> and 19.61 g kg<sup>-1</sup>, respectively (Gao *et al.*, 2017).

Spring maize was sown around May 1 at a row spacing of 0.5 m and a plant spacing of 0.3 m with plastic film mulching in 2015 and 2016. The mulching film and punch planter was used in the cropland, and one plastic film mulched three rows. The mulching area accounted for about 80% of the total in both years. The plastic film was a kind of transparent polyethylene film with a thickness of 8 µm, and did not visibly deteriorate until the harvest time. Base fertilization was consistent with the practice of local farmers (276 kg N ha<sup>-1</sup>, 144 kg P<sub>2</sub>O<sub>5</sub> ha<sup>-1</sup>, and 60 kg K<sub>2</sub>O ha<sup>-1</sup>). Straw was chopped using automated machines and returned to the field at harvest time. Any straw that did not decompose during the non-growing season was completely mixed with the soil through tillage in late April of the following year (Gao *et al.*, 2017).

### Eddy covariance measurements

An eddy covariance system was installed near the central of the spring maize cropland under plastic film (100 m × 260 m). The information about the composition and installation of this eddy covariance system was shown in Gao *et al.* (2017). And the data processing of water vapor fluxes was described in Gao *et al.* (2018).

## Other measurements

The measuring instruments of air temperature ( $T_a$ ), relative humidity ( $H_a$ ), net radiation ( $R_n$ ), soil water content at 10-cm depth (SWC), wind speed ( $U$ ) and precipitation ( $P$ ) were described in Gao *et al.* (2018). We used the manual method to measure the green leaf area index (GLAI) during the growing season (McKee, 1964; Gao *et al.*, 2018). Daily  $E$  was measured by ten micro-lysimeters made from polyvinyl chloride (PVC) tubes with a diameter of 10 cm and a height of 15 cm during the growing season, four micro-lysimeters were installed within bare soil between two films, and the remaining micro-lysimeters were installed under the film. The micro-lysimeters were reinstalled within 1 day after precipitation or on the third day of continuous measurements. Daily  $E$  at each micro-lysimeter was obtained as the difference between the weights measured by an electronic scale with the precision of 0.1 g at sunset, and weighted averaged as daily  $E$  in the spring maize field (Gao *et al.*, 2017).

## Non-mulching field

We also used eddy covariance system combined with micro-lysimeters to measure  $ET$  and its components in a non-mulching rainfed spring maize field in Shouyang site. The agricultural practices except for plastic film mulching in the non-mulching field were the same as the field under plastic film. The detailed information of  $ET$  and its components in the non-mulching field were shown in Gao *et al.* (2018).

## Parameter calculation

Following Alberto *et al.* (2014),  $ET$  was calculated as follows:

$$ET = \frac{LE}{2500 - 2.4T_a}$$

where  $LE$  is the latent heat flux ( $W\ m^{-2}$ ) and  $T_a$  is the air temperature ( $^{\circ}C$ ). The  $ET_0$  was calculated according to Allen *et al.* (1998):

$$ET_0 = \frac{0.408\Delta(R_n - G) + 900U \cdot \gamma \cdot VPD / (T_a + 273.3)}{\Delta + \gamma(1 + 0.34U)}$$

where  $R_n$  is the net radiation ( $MJ\ m^{-2}\ d^{-1}$ ),  $G$  is the soil heat flux ( $MJ\ m^{-2}\ d^{-1}$ ),  $U$  is the wind speed ( $m\ s^{-1}$ ),  $\gamma$  is the psychrometric constant ( $kPa\ ^{\circ}C^{-1}$ ),  $VPD$  is the vapor pressure deficit ( $kPa$ ), and  $\Delta$  is the slope of the water vapor pressure curve ( $kPa\ ^{\circ}C^{-1}$ ).

The crop coefficient ( $K_c$ ), soil water evaporation coefficient ( $K_e$ ), and basal crop coefficient ( $K_{cb}$ ) were given by Allen *et al.* (1998):

$$K_c = \frac{ET}{ET_0}; \quad K_e = \frac{E}{ET_0}; \quad K_{cb} = \frac{T}{K_s \cdot ET_0}$$

where  $K_s$  is soil water stress coefficient, and calculated according to Ding *et al.* (2013).

## Results

### Abiotic factors and GLAI

The abiotic factors and GLAI had similar general trends in both years, except for  $P$  and SWC (Fig. 1). The dynamics of daily  $R_n$  and  $T_a$  accorded with the quadratic curve, peaking at  $\sim 18\ MJ\ m^{-2}\ d^{-1}$  and  $\sim 25\ ^{\circ}C$ , respectively (Figs. 1a and 1b). With the coming of summer monsoon at the end of June, daily  $H_a$ ,  $U$ , and  $VPD$  generally increased, decreased, and decreased, respectively (Figs. 1c, 1d, and 1e). After each  $P$ , SWC increased suddenly and then decreased gradually, and total  $P$  was 386 and 461 mm in 2015 and 2016, respectively (Fig. 1f). The period from seed-sowing date (1 May in both years) to canopy dying date (7 October in 2015; 4 October in 2016) was defined as the growing season, and the GLAI peak marked the end of the canopy-increasing stage and the beginning of the canopy-decreasing stage. The peak values of GLAI were  $4.17\ m^2\ m^{-2}$  and  $3.76\ m^2\ m^{-2}$  on 24 July in 2015 and 31 July in 2016, respectively (Fig. 1g).

### ET and its components

Seasonal variations in  $ET_0$ ,  $ET$ ,  $E$ , and  $T$  in 2015 and 2016 are shown in Fig. 2. The daily  $ET_0$  displayed a parabolic trend, peaking in the canopy-increasing stage (Fig. 2a). The daily  $E$  was relatively small during the growing season (Fig. 2b). The daily  $T$  increased dramatically in the canopy-increasing stage, and then declined significantly in the canopy-decreasing stage (Fig. 2c). The daily  $ET$  trend was similar to that of daily  $T$  during the growing season, and was very small during the non-growing season (Fig. 2b). The daily  $ET$  and its components were disturbed by weather conditions; *i.e.*, they decreased sharply on cloudy and rainy days, and increased dramatically after those days. The relationships between daily GLAI and  $E/ET$  were logarithmic equations in the canopy-increasing and -decreasing stages (Fig. 3). These relationships were used to interpolate the miss data of daily  $E$  and  $T$  in the spring maize field under plastic film (Figs. 2b and 2c).

The  $P$  and  $ET$  were much lower in the non-growing season than in the growing season (Table 1).

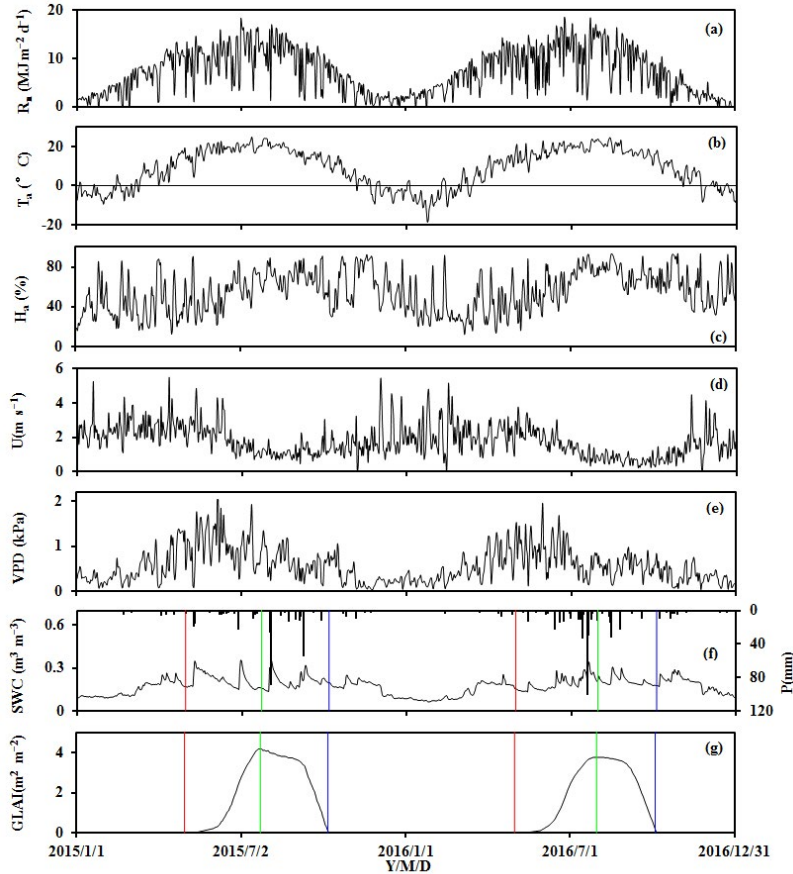


**Figure 1.** Seasonal variations in abiotic factors [(a) net radiation ( $R_n$ ), (b) air temperature ( $T_a$ ), (c) air relative humidity ( $H_a$ ), (d) wind speed ( $U$ ), (e) vapor pressure deficit ( $VPD$ ), (f) precipitation ( $P$ ), and soil water content at 10-cm depth ( $SWC$ )] and (g) green leaf area index ( $GLAI$ ) in 2015 and 2016. The periods between the red and green lines and between the green and blue lines are the canopy-increasing and -decreasing stages, respectively, in each year.

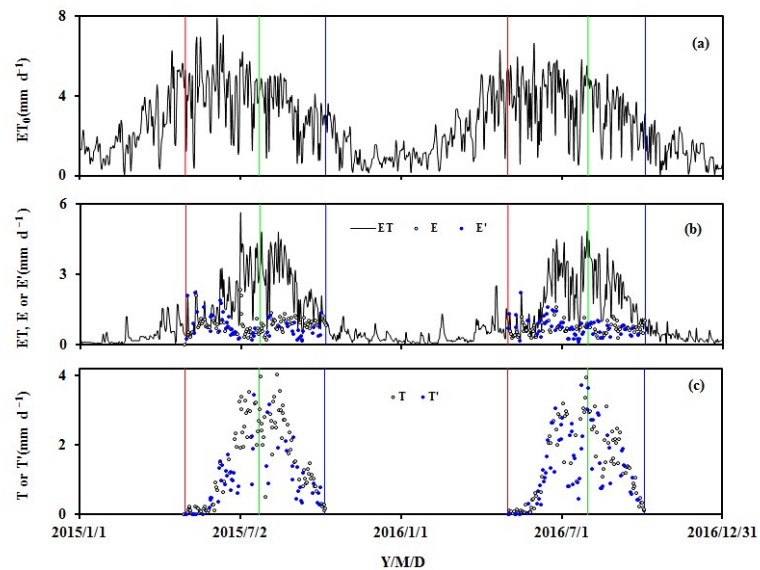


**Figure 2.** Seasonal variations in (a) reference crop evapotranspiration ( $ET_0$ ), (b) evapotranspiration ( $ET$ ) and soil evaporation ( $E$ ), and (c) crop transpiration ( $T$ ) in 2015 and 2016.  $E'$  and  $T'$  are the interpolated  $E$  and  $T$ , respectively, according to the relationships in Fig. 5. The periods between the red and green lines and between the green and blue lines are the canopy-increasing and -decreasing stages, respectively, in each year.

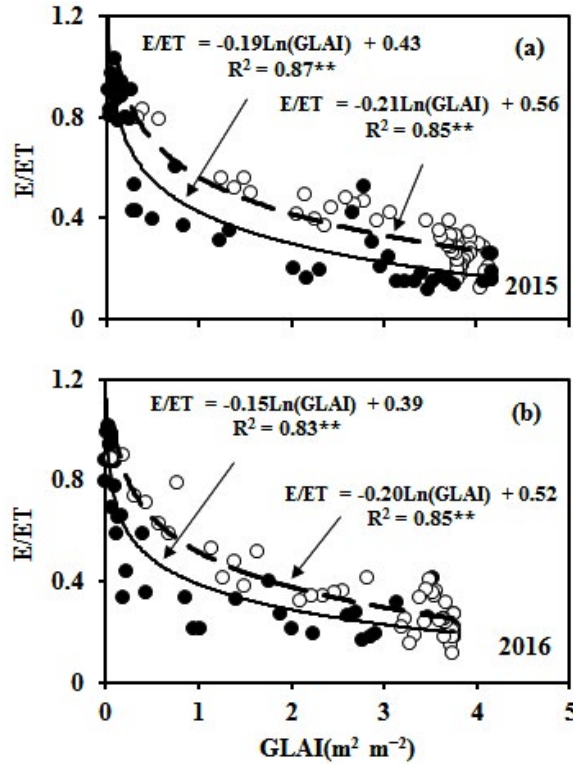


**Figure 3.** Relationships between green leaf area index (GLAI) and the ratio of daily soil evaporation to evapotranspiration (E/ET) in the canopy-increasing stage (solid symbols) and the canopy-decreasing stage (open symbols) in 2015 and 2016. \*\* represents significance level  $p < 0.001$ .

E values in the growing season were 123 and 107 mm, and accounted for 36% and 33% of ET in the growing season in the field under plastic film in 2015 and 2016, respectively. The water balance values were -5 and 78 mm in the growing season and -39 and -25 mm in the non-growing season in 2015 and 2016, respectively. These suggest that soil water increased only during the growing season in 2016. Water balance and ET partitions in the non-mul-

ching spring maize field at Shouyang site was also shown in Table 1. Compared to the field under plastic film, E and T values in the growing season in the non-mulching field were higher and lower respectively. Over the 2 years, total ET in the non-mulching field was greater than that in the field under plastic film by 30 mm. And the annual water balance values in the non-mulching field were -28 and 24 mm in 2015 and 2016, respectively.

**Table 1.** Evapotranspiration (ET) partitions and water balance of the spring maize field under plastic film mulching and the non-mulching spring maize field at the Shouyang site during the growing and non-growing seasons in 2015 and 2016.

Field	Year	Period	ET (mm)	P (mm)	Water balance (mm)	T (mm)	E (mm)	E/ET
Mulching	2015	Growing season	335	337	2	214	121	0.36
		Non-growing season	86	49	-37	-	-	-
	2016	Growing season	316	400	78	211	105	0.33
		Non-growing season	84	61	-23	-	-	-
Non-mulching <sup>[a]</sup>	2015	Growing season	338	337	-1	200	138	0.40
		Non-growing season	76	49	-27	-	-	-
	2016	Growing season	350	400	50	197	153	0.43
		Non-growing season	87	61	-26	-	-	-

<sup>[a]</sup> Water balance and ET partitions in the non-mulching spring maize field have been reported by Gao *et al.* (2018).

Seasonal variations in  $K_c$ ,  $K_e$ , and  $K_{cb}$  in 2015 and 2016 are shown in Fig. 4. The daily  $K_c$  in the non-growing season was generally low, and increased sharply after P (Fig. 4a). The daily  $K_c$  and  $K_{cb}$  gradually increased in the canopy-increasing stage and then declined in the canopy-decreasing stage, and was disturbed by P (Figs. 4a and 4b). The peak values of daily  $K_c$  and  $K_{cb}$  during the growing season appeared earlier in 2016 than in 2015. The daily  $K_c$  was generally low during the growing season, and was also disturbed by P (Fig. 4a). P had a stronger effect on daily  $K_c$  and  $K_e$  than on daily  $K_{cb}$  in the growing season. The monthly average  $K_c$ ,  $K_e$ , and  $K_{cb}$  in the growing season, and average  $K_c$  in the non-growing season in 2015 and 2016 are shown in Table 2.

Regardless of the effect of P on daily  $K_c$ ,  $K_e$ , and  $K_{cb}$ , the effects of GLAI on daily  $K_c$ ,  $K_e$ , and  $K_{cb}$  in the canopy-increasing and -decreasing stages in 2015 and 2016 are shown in Fig. 5. The data from rainy days or the three following days were removed from the database of daily  $K_c$ ,  $K_e$ , whereas the data from rainy days and one following day were removed from the database of daily  $K_{cb}$ , mainly because water evaporated more quickly from plant surfaces than the soil surface after rain. The daily  $K_c$  in the canopy-increasing stage increased with increasing GLAI when GLAI was less than  $\sim 3 \text{ m}^2 \text{ m}^{-2}$ , whereas in the canopy-decreasing stage it decreased linearly with decreasing GLAI (Figs. 5a and 5b). The daily  $K_e$  in the canopy-increasing stage was insensitive to GLAI, but increased linearly with decreasing GLAI in the canopy-decreasing stage (Figs. 5c and 5d). There was an exponential relationship between daily  $K_{cb}$  and GLAI in the canopy-increasing stage, whereas in the canopy-decreasing stage daily  $K_{cb}$  decreased linearly with decreasing GLAI (Figs. 5e and 5f). At equivalent GLAI, daily  $K_c$  and  $K_{cb}$  were usually higher in the canopy-decreasing and -increasing stages, respectively.

## Abiotic factors and GLAI controlling ET and its components

As shown in Table 3, the growing season daily ET and T were mainly controlled by  $R_n$ , followed by GLAI ( $p < 0.001$ ). And  $H_a$  and VPD also had an impact on growing season daily T ( $p < 0.05$ ). The growing season daily E was mainly controlled by  $R_n$ , followed by SWC ( $p < 0.001$ ), and had negative correlations with GLAI in 2016 ( $p < 0.05$ ). The non-growing season daily ET were mainly controlled by  $R_n$  ( $p < 0.001$ ), and was also influenced by SWC ( $p < 0.001$ ) and U ( $p < 0.05$ ) in 2015.

As shown in Table 4, the selected factors (those with  $p < 0.001$  in Table 3) predicted the growing season daily ET and T variations well with goodness-of-fit values of 0.79–0.80. Changes in selected factors also explained 43–52% of the variations in the non-growing season daily ET and growing season daily E.

## Discussion

The growing season ET was 342 mm (daily average of  $2.24 \text{ mm d}^{-1}$ ) and 322 mm (daily average of  $2.11 \text{ mm d}^{-1}$ ) in the field under plastic film in 2015 and 2016, respectively (Table 1). Compared to irrigated spring maize fields under plastic film in northwest China (Ding *et al.*, 2013; Li *et al.*, 2013; Zhang *et al.*, 2016), the water consumption was lower in this study. Suyker & Verma (2009) observed total ET values ranging from 502 to 586 mm and daily average ET values ranging from  $3.02$  to  $3.62 \text{ mm d}^{-1}$  in irrigated spring maize croplands in Nebraska, USA, those values were also higher than those in our study. The different agricultural practices and climate conditions in our study area could be the main reason that our results differed from those of published studies in which the eddy

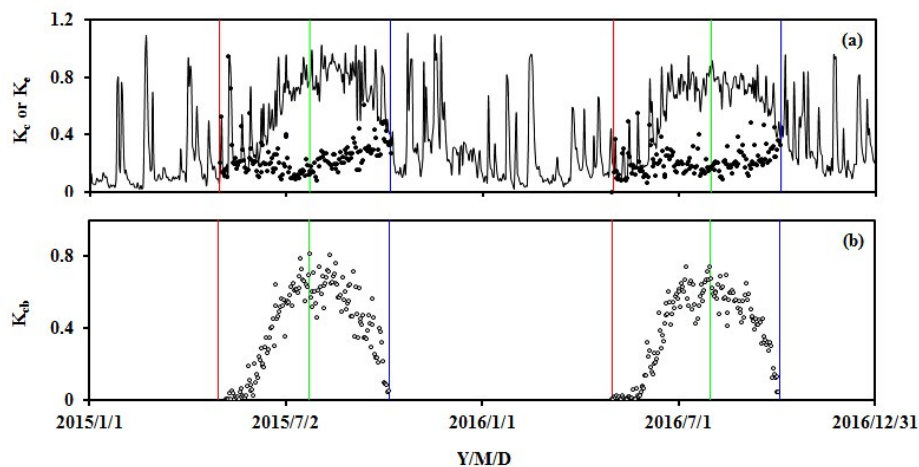


**Figure 4.** Seasonal variations in (a) crop coefficient ( $K_c$ ) and soil water evaporation coefficient ( $K_e$ ), and (b) basal crop coefficient ( $K_{cb}$ ) in 2015 and 2016. The periods between the red and green lines and between the green and blue lines are the canopy-increasing and -decreasing stages, respectively, in each year.

**Table 2.** Monthly average crop coefficient ( $K_c$ ), basal crop coefficient ( $K_e$ ), and soil water evaporation coefficient ( $K_{cb}$ ) in the growing season, and average  $K_c$  in the non-growing season in 2015 and 2016.

Year	Period	Month	$K_c$	$K_e$	$K_{cb}$
2015	Growing season	May	0.31	0.30	0.01
		June	0.49	0.19	0.20
		July	0.76	0.16	0.62
		August	0.85	0.23	0.62
		September <sup>[a]</sup>	0.74	0.32	0.42
	Non-growing season	–	0.22	–	–
2016	Growing season	May	0.20	0.18	0.02
		June	0.59	0.22	0.37
		July	0.79	0.18	0.61
		August	0.76	0.20	0.56
		September <sup>[b]</sup>	0.65	0.25	0.40
	Non-growing season	–	0.23	–	–

<sup>[a]</sup> From 1 September to 7 October. <sup>[b]</sup> From 1 September to 4 October.

covariance system was also used to measure water flux. Previous studies of using the water balance method in rainfed spring maize croplands under plastic film on the Loess Plateau have reported the growing season ET values of 358–373 mm (Liu *et al.*, 2010b), 351–369 mm (Bu *et al.*, 2013), and 331–376 mm (Zhou *et al.*, 2009), which

are comparable to the corresponding values in our study. Compared to the non-mulching field, the growing season ET in the field under plastic film was lower by 3 and 34 mm in 2015 and 2016 at our site, respectively (Table 1). Those results agree with previous studies on the Loess Plateau (Liu *et al.*, 2010b; Bu *et al.*, 2013), suggesting

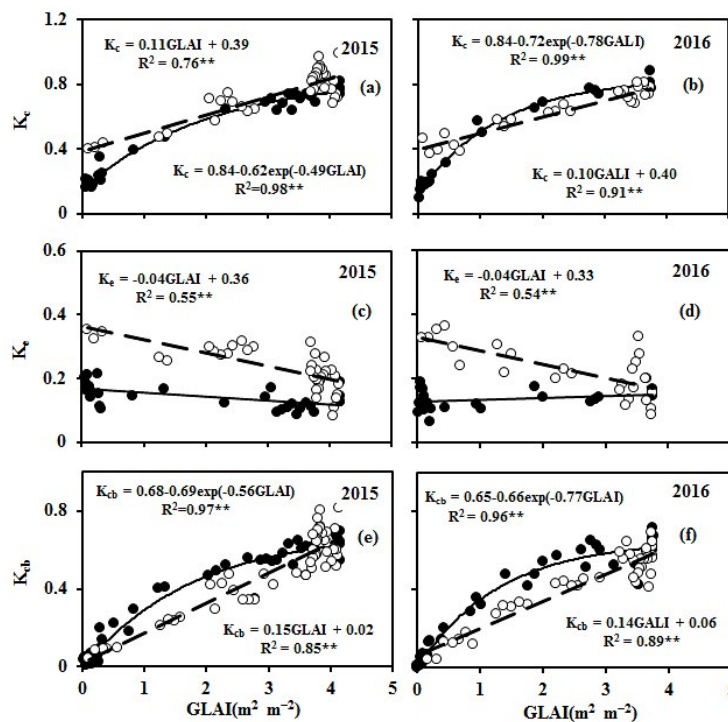


**Figure 5.** Relationships between green leaf area index (GLAI) and crop coefficient ( $K_c$ ), soil water evaporation coefficient ( $K_e$ ), and basal crop coefficient ( $K_{cb}$ ) in the canopy-increasing stage (solid symbols) and the canopy-decreasing stage (open symbols) in 2015 and 2016. \*\* represents significance level  $p < 0.001$ . The  $K_c$  and  $K_e$  data on rainy days and three days after rain, and  $K_{cb}$  data on rainy day and one day after rain are not shown in the figure.

**Table 3.** Partial correlation coefficients between daily water fluxes (ET, T, and E) and green leaf area index (GLAI) and abiotic factors ( $R_n$ ,  $T_a$ , VPD,  $H_a$ , U, P, and SWC) in 2015 and 2016.

Water fluxes	Year	Period	$R_n$	$T_a$	VPD	$H_a$	U	P	SWC	GLAI
ET	2015	Growing season	0.74**	-0.08	0.16	0.16	-0.01	-0.01	0.02	0.47**
		Non-growing season	0.46**	0.01	-0.01	0.13	0.24*	0.07	0.42**	-
	2016	Growing season	0.77**	-0.10	0.16	0.17	0.05	-0.10	0.09	0.34**
		Non-growing season	0.69**	0.11	-0.05	-0.15	0.22	0.05	0.19	-
T	2015	Growing season	0.63**	-0.05	0.22*	0.22*	-0.05	-0.02	-0.15	0.60**
	2016	Growing season	0.71**	-0.10	0.24*	0.24*	0.09	0.00	-0.06	0.50**
E	2015	Growing season	0.65**	-0.10	-0.06	-0.07	0.08	0.02	0.31**	-0.18
	2016	Growing season	0.63**	-0.03	-0.05	-0.07	-0.06	-0.02	0.30**	-0.25*

\*, \*\*: significance level  $p < 0.05$  and  $p < 0.001$ , respectively. Data during the non-growing season were chosen from the period when  $T_a > 0^\circ\text{C}$

that plastic film mulching could decrease ET in rainfed spring maize fields.

On an annual scale, water balance in the field under plastic film was -44 and 53 mm in 2015 and 2016, respectively (Table 1). Similar to our study, ET consumed almost all P (annual ET/P between 0.94 and 1.28) in a rainfed agroecosystem in Nebraska, USA (Suyker & Verma, 2009). Although straw-returning had been used in the field under plastic film, the non-growing season soil water decreased by 39 and 25 mm in 2015 and 2016, respectively (Table 1), implying that it may be critical to optimize agricultural practices for water management during the non-growing season. The non-growing season soil water in the non-mulching field also decreased by 23 and 26 mm in 2015 and 2016, respectively (Table 3), which are comparable to the field under plastic film, mainly because plastic film was destroyed by the machine when the straw was returned to the field. Zhang *et al.* (2016) also

proved that the non-growing season soil water decreased in irrigated spring maize croplands in northwest China. However, the non-growing season soil water increased by 43–169 mm in a rainfed maize–soybean agroecosystem (Suyker & Verma, 2009), where the non-growing season P (194–332 mm) was much greater than at our study site (Table 1). In addition, about 20% of annual ET occurred in the non-growing season at our site (Table 1), which was comparable to percentages for a rainfed maize–soybean agroecosystem (20–26%, Suyker & Verma, 2009), and irrigated spring maize fields (~15%, Zhang *et al.*, 2016).

The E consumed 36% and 33% of growing season ET in 2015 and 2016, respectively (Table 1), indicating that the growing season ET was mainly consumed by T in the field under plastic film. The growing season E/ET ratios were comparable to that in a winter wheat cropland (0.32, Liang *et al.*, 2011), but lower than that in a summer maize cropland in northwest China (0.44–0.53, Wang *et al.*,

**Table 4.** Regression results of multi-factor linear model between daily water fluxes (ET, T, and E) and green leaf area index (GLAI) and abiotic factors, selected according to significance level  $p < 0.001$  (Table 3).

Water fluxes	Year	Period	Multi-factor linear model	$R^2$
ET	2015	Growing season	$0.20 \times R_n + 0.35 \times \text{GLAI} - 0.69$	0.80**
		Non-growing season	$0.05 \times R_n + 7.39 \times \text{SWC} - 1.18$	0.52**
	2016	Growing season	$0.20 \times R_n + 0.36 \times \text{GLAI} - 0.79$	0.80**
		Non-growing season	$0.07 \times R_n + 0.13$	0.43**
T	2015	Growing season	$0.14 \times R_n + 0.47 \times \text{GLAI} - 1.07$	0.79**
	2016	Growing season	$0.15 \times R_n + 0.41 \times \text{GLAI} - 1.02$	0.79**
E	2015	Growing season	$0.06 \times R_n + 3.28 \times \text{SWC} - 0.56$	0.50**
	2016	Growing season	$0.05 \times R_n + 0.02 \times \text{SWC} - 0.14$	0.45**

\*\* : significance level  $p < 0.001$ .



2007). Compared to the non-mulching field, the growing season E/ET, E, and T in the field under plastic film were lower, lower, and higher, respectively (Table 1). Those results indicate that plastic film decrease E, increase T, and promote the distribution of ET to the T, and finally stimulates the growth and development of crops, which is in agreement with the published studies (Liu *et al.*, 2010b; Bu *et al.*, 2013). Daily E/ET decreased logarithmically with increasing GLAI (Fig. 3), indicating that seasonal variations in GLAI controlled daily E/ET during the growing season. Similar relationships between GLAI and daily E/ET were also found in winter wheat and summer maize croplands in northwest China (Kang *et al.*, 2003; Wang *et al.*, 2007). At the same GLAI, daily E/ET was lower in the canopy-increasing stage than in the canopy-decreasing stage (Fig. 3); we suspect the higher transpiration rate of GLAI in the canopy-increasing stage may be responsible for this phenomenon.

The peak monthly average  $K_c$  values were 0.85 and 0.79 in August 2015 and July 2016, respectively (Table 2). Mid-season average  $K_c$  values were between 0.71 and 0.90 in a rainfed spring maize cropland in Nebraska, USA (Suyker & Verma, 2009), and from 0.85 to 0.90 in an irrigated cotton field in northwest China (Yang *et al.*, 2016), values that are comparable to our results. However, average  $K_c$  values during periods of vigorous growth were usually  $> 1$  in irrigated spring maize croplands in northwest China (Li *et al.*, 2008; Jiang *et al.*, 2014) and Nebraska, USA (Suyker & Verma, 2009). The daily  $K_c$  at our site increased with increasing GLAI until the GLAI threshold ( $\sim 3 \text{ m}^2 \text{ m}^{-2}$ ) in the canopy-increasing stage (Figs. 5a and 5b). These results are in agreement with those of Zhang *et al.* (2016) for irrigated spring maize croplands and Kang *et al.* (2003) for a summer maize field. These results indicate that ET is dramatically affected by GLAI when GLAI is below a certain threshold value in the canopy-increasing stage. The daily  $K_c$  at our site decreased linearly with decreasing GLAI in the canopy-decreasing stage (Figs. 5a and 5b). Yuan *et al.* (2014) and Suyker & Verma (2008) also reported nearly linear relationships between GLAI and daily  $K_c$  during the canopy-decreasing stage in a desert ecosystem and in an irrigated agricultural ecosystem, respectively. The curvature of the exponential curve between GLAI and daily  $K_c$  was relatively low in the canopy-increasing stage in 2015 (Fig. 5a), possibly because of soil water stress due to lower P in this stage (Fig. 1f), resulting in ET that was more dependent on GLAI and with a higher partial correlation coefficient (Table 3). The relationships between daily  $K_{cb}$  and GLAI in the canopy-increasing and -decreasing stages were similar to those between daily  $K_c$  and GLAI (Figs. 5e and 5), since T was the main component of ET, and there were similar seasonal variations in T and ET. E was relatively stable during the growing season (Fig. 2b);  $ET_0$  was also relatively stable during the canopy-increasing stage, but

decreased in the canopy-decreasing stage (Fig. 2a), resulting in daily  $K_c$  values that were insensitive to GLAI in the canopy-increasing stage but increased linearly with decreasing GLAI in the canopy-decreasing stage (Figs. 5c and 5d).

Because abiotic factors, such as  $R_n$ ,  $T_a$ , U, and VPD calculated from  $T_a$  and  $H_a$ , are the variables to calculate  $ET_0$  (Allen *et al.*, 1998), they have an important effect on seasonal variations in daily ET during the growing season reported in many previous studies (Li *et al.*, 2008; Alberto *et al.*, 2014; Zhang *et al.*, 2016). In this study, daily ET and its components was most influenced by  $R_n$ , indicating the energy supply plays a key role in cropland water consumption on the Loess Plateau. As abiotic factors influence T by acting on green leaves, daily T and ET were also controlled by GLAI at our site (Table 3), which is in agreement with the results in a maize field in the Philippines (Alberto *et al.*, 2014). We suspect higher GLAI combined with higher  $ET_0$ , may be the main reason for the higher growing season ET value in 2015, although the growing season P was higher in 2016. The water sources for T and E are the root zone (0–100 cm) and surface soil (0–10 cm), respectively (Ding *et al.*, 2013; Li *et al.*, 2013). Consequently, SWC had a small but significant effect on daily T and E, respectively, in this study (Table 3). Although P had little influence on daily ET and its components (Table 3), the water in the soil and on plant surfaces evaporates very easily after a P event, resulting in a sharp increase in daily ET and its components, daily  $K_c$  and its components on sunny days following P events.

In this study, almost all P was consumed by ET, implying that the groundwater and runoff were not replenished from rainfed croplands on the Loess Plateau. The daily  $K_c$  and its components reacted differently to GLAI in the canopy-increasing and -decreasing stages, suggesting that crop growth had different effects on ET in different growth stages. Future studies should focus on the response of ET to climate change in relation to energy partitioning, carbon uptake and water use efficiency in rainfed croplands on the Loess Plateau.

## References

- Alberto MCR, Quilty JR, Buresh RJ, Wassmann R, Haidar S, Correa Jr. TQ, Sandro JM, 2014. Actual evapotranspiration and dual crop coefficients for dry-seeded rice and hybrid maize grown with overhead sprinkler irrigation. *Agric Water Manage* 136: 1-12. <https://doi.org/10.1016/j.agwat.2014.01.005>
- Allen RG, Pereira LS, Raes D, Smith M, 1998. Crop evapotranspiration: guide-lines for computing crop requirements. *Irrig Drain Paper No. 56*. FAO, United Nations, Rome..

- Bu LD, Liu JL, Lou SS, Chen XP, Li SQ, Hill RL, Zhao Y, 2013. The effects of mulching on maize growth, yield and water use in a semi-arid region. *Agric Water Manage* 123: 71-78. <https://doi.org/10.1016/j.agwat.2013.03.015>
- Ding RS, Kang SZ, Li FS, Zhang YQ, Tong L, 2013. Evapotranspiration measurement and estimation using modified Priestley-Taylor model in an irrigated maize field with mulching. *Agric For Meteorol* 168: 140-148. <https://doi.org/10.1016/j.agrformet.2012.08.003>
- FAO, 2011. The state of the world's land and water resources for food and agriculture (SOLAW)- Managing systems at risk. FAO, United Nations, Rome and Earthscan, London.
- Gao X, Gu FX, Mei XR, Hao WP, Li HR, Gong DZ, 2017. Carbon exchange of a rainfed spring maize cropland under plastic film mulching with straw returning on the Loess Plateau, China. *Catena* 158: 298-308. <https://doi.org/10.1016/j.catena.2017.07.015>
- Gao X, Mei XR, Gu FX, Hao WP, Gong DZ, Li HR, 2018. Evapotranspiration partitioning and energy budget in a rainfed spring maize field on the Loess Plateau, China. *Catena* 166: 249-259. <https://doi.org/10.1016/j.catena.2018.04.008>
- Jiang XL, Kang SZ, Tong L, Li FS, Li DH, Ding RS, Qiu RJ, 2014. Crop coefficient and evapotranspiration of grain maize modified by planting density in an arid region of northwest China. *Agric Water Manage* 142: 135-143. <https://doi.org/10.1016/j.agwat.2014.05.006>
- Kang SZ, Gu BJ, Du TS, Zhang JH, 2003. Crop coefficient and ratio of transpiration to evapotranspiration of winter wheat and maize in a semi-humid region. *Agric Water Manage* 59: 239-254. [https://doi.org/10.1016/S0378-3774\(02\)00150-6](https://doi.org/10.1016/S0378-3774(02)00150-6)
- Kool D, Agam N, Lazarovitch N, Heitman JL, Sauer TJ, Ben-Gal A, 2014. A review of approaches for evapotranspiration partitioning. *Agric For Meteorol* 184: 56-70. <https://doi.org/10.1016/j.agrformet.2013.09.003>
- Li SE, Kang SZ, Li FS, Zhang L, 2008. Evapotranspiration and crop coefficient of spring maize with plastic mulch using eddy covariance in northwest China. *Agric Water Manage* 95: 1214-1222. <https://doi.org/10.1016/j.agwat.2008.04.014>
- Li SE, Kang SZ, Zhang L, Ortega-Farias S, Li FS, Du TS, Tong L, Wang SF, Ingman M, Guo WH, 2013. Measuring and modeling maize evapotranspiration under plastic film-mulching condition. *J Hydrol* 503: 153-168. <https://doi.org/10.1016/j.jhydrol.2013.07.033>
- Liang WQ, Cai H, Wang J, 2011. Research of evapotranspiration and evaporation for winter wheat. *J Irrig Drain* 30: 93-96. (In Chinese with English abstract).
- Liu CA, Jin SL, Zhou LM, Jia Y, Li FM, Xiong YC, Li XG, 2009. Effects of plastic film mulch and tillage on maize productivity and soil parameters. *Eur J Agron* 31: 241-249. <https://doi.org/10.1016/j.eja.2009.08.004>
- Liu Y, Li SQ, Chen F, Yang SJ, Chen XP, 2010a. Soil water dynamics and water use efficiency in spring maize (*Zea mays* L.) fields subjected to different water management practices on the Loess Plateau, China. *Agric Water Manage* 97: 769-775. <https://doi.org/10.1016/j.agwat.2010.01.010>
- Liu Y, Yang SJ, Li SQ, Chen XP, Chen F, 2010b. Growth and development of maize (*Zea mays* L.) in response to different field water management practices: Resource capture and use efficiency. *Agric For Meteorol* 150: 606-613. <https://doi.org/10.1016/j.agrformet.2010.02.003>
- McKee GW, 1964. A coefficient for computing leaf area in hybrid corn. *Agron J* 56: 240-241. <https://doi.org/10.2134/agronj1964.00021962005600020038x>
- Miao QF, Rosa RD, Shi HB, Paredes P, Zhu L, Dai JX, Gonçalves JM, Pereira LS, 2016. Modeling water use, transpiration and soil evaporation of spring wheat-maize and spring wheat-sunflower relay intercropping using the dual crop coefficient approach. *Agric Water Manage* 165: 211-229. <https://doi.org/10.1016/j.agwat.2015.10.024>
- Sen Z, 2004. Solar energy in progress and future research trends. *Prog Energy Combust Sci* 30: 367-416. <https://doi.org/10.1016/j.peccs.2004.02.004>
- Suyker AE, Verma SB, 2008. Interannual water vapor and energy exchange in an irrigated maize-based agroecosystem. *Agric For Meteorol* 148: 417-427. <https://doi.org/10.1016/j.agrformet.2007.10.005>
- Suyker AE, Verma SB, 2009. Evapotranspiration of irrigated and rainfed maize-soybean cropping systems. *Agric For Meteorol* 149: 443-452. <https://doi.org/10.1016/j.agrformet.2008.09.010>
- Taylor AM, Amiro BD, Fraser TJ, 2013. Net CO<sub>2</sub> exchange and carbon budgets of a three-year crop rotation following conversion of perennial lands to annual cropping in Manitoba, Canada. *Agric For Meteorol* 182: 67-75. <https://doi.org/10.1016/j.agrformet.2013.07.008>
- Wang J, Cai HJ, Kang YX, Chen F, 2007. Ratio of soil evaporation to the evapotranspiration for summer maize field. *T CSAE* 23: 17-22. (In Chinese with English abstract).
- Wever LA, Flanagan LB, Carlson PJ, 2002. Seasonal and interannual variation in evapotranspiration, energy balance and surface conductance in northern temperate grassland. *Agric For Meteorol* 112: 31-49. [https://doi.org/10.1016/S0168-1923\(02\)00041-2](https://doi.org/10.1016/S0168-1923(02)00041-2)
- Wu CL, Shukla S. 2014. Eddy covariance-based evapotranspiration for a subtropical wetland. *Hydrol Process* 28: 5879-5896. <https://doi.org/10.1002/hyp.10075>
- Yang XY, Asseng S, Wong MTF, Yu Q, Li J, Liu E, 2013. Quantifying the interactive impacts of global dimming and warming on wheat yield and water use in China.

- Agric For Meteorol 182-183: 342-351. <https://doi.org/10.1016/j.agrformet.2013.07.006>
- Yang PJ, Hu HC, Tian FQ, Zhang Z, Dai C, 2016. Crop coefficient for cotton under plastic mulch and drip irrigation based on eddy covariance observation in an arid area of northwestern China. *Agric Water Manage* 171: 21-30. <https://doi.org/10.1016/j.agwat.2016.03.007>
- Yuan GF, Zhang P, Shao MA, Luo Y, Zhu C, 2014. Energy and water exchanges over a riparian *Tamarix* spp. stand in the lower Tarim River basin under a hyper-arid climate. *Agric For Meteorol* 194: 144-154. <https://doi.org/10.1016/j.agrformet.2014.04.004>
- Zhang YY, Zhao WZ, He JH, Zhang K, 2016. Energy exchange and evapotranspiration over irrigated seed maize agroecosystems in a desert-oasis region, northwest China. *Agric For Meteorol* 223: 48-59. <https://doi.org/10.1016/j.agrformet.2016.04.002>
- Zhao P, Li SE, Li FS, Du TS, Tong L, Kang SZ, 2015. Comparison of dual crop coefficient method and Shuttleworth-Wallace model in evapotranspiration partitioning in a vineyard of northwest China. *Agric Water Manage* 160: 41-56. <https://doi.org/10.1016/j.agwat.2015.06.026>
- Zhou LM, Li FM, Jin SL, Song YJ, 2009. How two ridges and the furrow mulched with plastic film affect soil water, soil temperature and yield of maize on the semiarid Loess Plateau of China. *Field Crops Res* 113: 41-47. <https://doi.org/10.1016/j.fcr.2009.04.005>